Prolonged High-Fat Feeding Enhances Aortic ^{18}F-FDG and ^{99m}Tc-Annexin A5 Uptake in Apolipoprotein E-Deficient and Wild-Type C57BL/6J Mice

Yan Zhao[1], Yuji Kuge[2,3], Songji Zhao[1,2], H. William Strauss[4], Francis G. Blankenberg[5], and Nagara Tamaki[1]

[1]Department of Nuclear Medicine, Graduate School of Medicine, Hokkaido University, Sapporo, Japan; [2]Department of Tracer Kinetics and Bioanalysis, Graduate School of Medicine, Hokkaido University, Sapporo, Japan; [3]Department of Molecular Imaging, Graduate School of Medicine, Hokkaido University, Sapporo, Japan; [4]Department of Nuclear Medicine, Memorial Sloan-Kettering Cancer Center, New York, New York; and [5]Department of Pediatric Radiology, Stanford University School of Medicine, Palo Alto, California

^{18}F-FDG, a marker of the enhanced metabolism characteristic of activated inflammatory cells, and ^{99m}Tc-annexin A5, a marker of apoptosis, are both widely believed to be useful for the imaging of unstable atheroma (rupture-prone vulnerable plaques [VP]). Serum cholesterol functions as a proinflammatory factor, driving the formation of VP, and affects the immune responses of aortic tissues systemically. It is therefore reasonable to postulate that prolonged cholesterol loading may alter the aortic uptake of these tracers. Here, we evaluated the aortic uptake of ^{18}F-FDG and ^{99m}Tc-annexin A5 in apolipoprotein E-deficient (apoE$^{-/-}$) and wild-type mice placed on high-fat diets. **Methods:** Male apoE$^{-/-}$ and wild-type (C57BL/6J) mice were maintained on high-fat diets after the age of 5 wk. Wild-type mice fed regular chow were used as controls. At the ages of 10, 18, and 25 wk (5–15 mice per group at each time point), mice were injected with ^{18}F-FDG or ^{99m}Tc-annexin A5 after 12 h of fasting. At 1 h after ^{18}F-FDG injection (or 2 h after ^{99m}Tc-annexin A5 injection), mice were sacrificed, and the aortas were removed for well-type scintillation counting of radioactivity. The results were expressed as percentage injected dose per gram of tissue and normalized by animal body weight [(ID%/g) × kg]. En face staining was then performed to assess the location and size (surface area) of the lipid pool within each aortic specimen. Concurrent blood samples were obtained to determine the plasma lipid profile of each group. **Results:** No atherosclerotic lesions were found in wild-type mice regardless of the diet, whereas the lesion area progressively increased with age in apoE$^{-/-}$ mice. Mean plasma cholesterol levels remained stable with the regular diet in wild-type mice (73–78 mg/dL) but increased with cholesterol feeding in wild-type mice (143–179 mg/dL) and in apoE$^{-/-}$ mice (>1,300 mg/dL). Aortic tracer uptake [(ID%/g) × kg] remained stable with the regular diet in wild-type mice (0.054–0.053 and 0.021–0.023 for ^{99m}Tc-annexin A5) but increased with cholesterol feeding in wild-type mice (0.164 for ^{18}F-FDG and 0.036 for ^{99m}Tc-annexin A5 at 25 wk) and in apoE$^{-/-}$ mice (0.249 for ^{18}F-FDG and 0.047 for ^{99m}Tc-annexin A5 at 25 wk). **Conclusion:** The accumulation of ^{18}F-FDG and ^{99m}Tc-annexin A5 in aortic tissues is influenced not only by the progression of atherosclerotic disease but also by cholesterol loading over time.

Key Words: atherosclerosis; apoptosis; inflammation; serum cholesterol levels

The spontaneous rupture of vulnerable plaques (VP) is a common cause of both myocardial and cerebral infarctions (*1,2*). The detection of VP is therefore clinically important for patient risk stratification and the delivery of early dietary interventions and lipid-lowering treatments. Nuclear imaging can noninvasively quantify 2 of the most important determinants of plaque vulnerability, namely, active inflammation (with ^{18}F-FDG PET) and apoptosis (with ^{99m}Tc-annexin A5 SPECT) (*3–7*).

Serum cholesterol, particularly oxidized low-density lipoprotein (LDL) cholesterol, acts as a proinflammatory factor (*8*) that increases the systemic levels of many immune system markers (*9,10*). For example, modified LDL stimulates endothelial cells to express monocyte chemotactic protein 1, which in turn recruits monocytes into the arterial wall (*11,12*). Monocyte chemotactic protein 1 also promotes the differentiation of infiltrating monocytes into macrophages and foam cells (*13*). Apoptosis of inflammatory and vascular smooth muscle cells of the arterial wall is an integral feature of the pathogenesis of VP (*14*). An increased rate of apoptosis in the diseased arterial wall is associated with high levels of circulating oxidized LDL (*15–17*). Elevated levels of serum cholesterol may therefore influence the extent of aortic plaque inflammation and apoptosis, leading to the increased uptake of ^{18}F-FDG and ^{99m}Tc-annexin A5, respectively. In this investigation, we attempted to determine the effects of

prolonged cholesterol loading on the aortic uptake of ^{18}F-FDG and ^{99m}Tc-annexin A5.

We used the apolipoprotein E-deficient (apoE$^{-/-}$) murine model of atherosclerosis (18). When fed a high-fat diet, apoE$^{-/-}$ mice develop severe hypercholesterolemia and atherosclerotic disease similar to human disease. In contrast, wild-type mice show only moderate hypercholesterolemia while on a high-fat diet. We evaluated the effects of serum cholesterol levels on the aortic uptake of ^{18}F-FDG and ^{99m}Tc-annexin A5 in both wild-type and apoE$^{-/-}$ mice placed on high-fat diets over time.

MATERIALS AND METHODS

Preparations of ^{18}F-FDG and ^{99m}Tc-Annexin A5

^{18}F-FDG was obtained from Hokkaido University Hospital, which produces the tracer for clinical use. Recombinant human annexin A5 derivatized with hydrazinonicotinamide was kindly donated by Theseus Imaging Corp. Hydrazinonicotinamide-annexin A5 was labeled with ^{99m}Tc by use of tricine as the coligand as described previously (specific activity: 4.8 MBq/μg of protein) (19).

Animal Studies

Animal care and all experimental procedures were performed with the approval of the Animal Care Committee at Hokkaido University. Studies were performed with male apoE$^{-/-}$ mice (5–14 per group) and male wild-type mice (C57BL/6J; 5–15 per group) obtained from Taconic Gnotobiotic Center and Clea Japan Inc., respectively. After the age of 5 wk, apoE$^{-/-}$ mice and wild-type mice were maintained on a high-fat, high-cholesterol diet (21% fat, 0.15% cholesterol, no cholate; diet TD88137 [Harland Teklad]) (ChD–apoE$^{-/-}$ mice and ChD–wild-type mice, respectively). Additional age-matched male wild-type mice were maintained on a laboratory chow basal diet (Oriental MF [Oriental Yeast Co. Ltd.]) for use as controls (normal diet–wild-type mice). All animals were kept on a 12-h light cycle with free access to food and water in a temperature-controlled facility at the Laboratory of Animal Experiments at Hokkaido University.

At the ages of 10, 18, and 25 wk, the animals were fasted, anesthetized with pentobarbital (0.025 mg/kg of body weight, intraperitoneally), and injected with either ^{18}F-FDG (18.5 MBq/mouse) or ^{99m}Tc-annexin A5 (18.5 MBq/mouse). The blood glucose levels of all animals were measured immediately before the injection. At 1 h after the ^{18}F-FDG injection or 2 h after the ^{99m}Tc-annexin A5 injection, blood samples (0.9–1.5 mL/mouse) were collected under deep pentobarbital anesthesia for subsequent analyses. Aortas were fixed by cardiac perfusion with a cold 0.1 M phosphate buffer solution (pH 7.4) and then a cold fixative (4% paraformaldehyde and 0.1 M phosphate buffer solution [pH 7.4]), removed, and weighed. Radioactivity in each aorta was measured in a well-type scintillation counter. The results were expressed as percentage injected dose per gram of tissue and normalized by animal body weight [(ID%/g) × kg].

Evaluation of Atherosclerotic Lesions

After radioactivity counting was complete, aortic specimens were longitudinally incised, mounted on clean glass slides, and stained with Oil Red O (Sigma) by use of the following protocol (20). In brief, each specimen was rinsed in 60% 2-propanol for 3 min, incubated in Oil Red O solution at 37°C for 40 min, destained in 60% 2-propanol for 6 min, and then mounted on a glass slide with aqueous mounting medium (Biomeda Corp.). Stained specimens were examined microscopically (BX50; Olympus), and the percentage of positively stained surface area for each aortic specimen was calculated.

Oil Red O staining and immunohistochemical staining with a mouse macrophage–specific antibody (Mac-2, clone m3/38; Cedarlane) were performed by use of standard procedures (20) with 5-μm-thick cryostat cross sections of aortic tissues from 4 additional mice at 25 wk of age in each group (ChD–apoE$^{-/-}$, ChD–wild-type, and normal diet–wild-type mice) to confirm the presence of atherosclerotic disease (Fig. 1) and macrophage infiltration (Supplemental Fig. 1) (supplemental materials are available online only at http://jnm.snmjournals.org).

Statistical Analysis

Numeric parameters were expressed as mean ± SD. To evaluate the effects of animal treatments (regular diet feeding, cholesterol feeding, and cholesterol feeding plus apolipoprotein E deficiency) or age (duration of treatment) on body weight, serum cholesterol levels, blood glucose levels, and aortic tracer uptake, the data were first tested with Bartlett's test for homogeneity of variance. If Bartlett's test confirmed homogeneity of variance, that is, a Bartlett's test value of greater than 0.05, then a 1-way ANOVA followed by a Bonferroni post hoc test was performed; if Bartlett's test indicated heterogeneity of variance, that is, a Bartlett's test value of less than 0.05 (cross-sectional comparisons for parameters; longitudinal comparisons for body weight and aortic ^{18}F-FDG uptake), then a nonparametric Kruskal–Wallis test followed by a Games–Howell multiple comparisons test was performed (Tables 1–3). A 2-way factorial ANOVA was performed to evaluate the degree of atherosclerotic lesion development with age in ChD–apoE$^{-/-}$ mice given ^{18}F-FDG and ^{99m}Tc-annexin A5 (Fig. 2).

A linear regression analysis correlating the percentages of aortic surface area occupied by atherosclerotic plaques with aortic tracer uptake in ChD–apoE$^{-/-}$ mice given ^{18}F-FDG and ^{99m}Tc-annexin A5 was performed (Fig. 3). The correlation between LDL cholesterol levels and aortic tracer uptake was assessed with the Spearman correlation coefficient by rank analysis in mice given ^{18}F-FDG and ^{99m}Tc-annexin A5 at each age (Supplemental Fig. 2).

A 2-tailed P value of less than 0.05 was considered statistically significant.

RESULTS

Body Weight, Serum Cholesterol Levels, and Blood Glucose Levels

Table 1 shows the age, body weight, and serum cholesterol levels for each group of treated mice. Body weight increased substantially with age in all treatment groups. ChD–apoE$^{-/-}$ mice showed the greatest gain in body weight, followed by ChD–wild-type and normal diet–wild-type mice. Severe hypercholesterolemia and moderate hypercholesterolemia were observed in ChD–apoE$^{-/-}$ and ChD–wild-type mice, respectively, throughout the experimental period. Total cholesterol and LDL cholesterol levels were significantly higher in ChD–apoE$^{-/-}$ mice than in ChD–wild-type and normal diet–wild-type mice. Total cholesterol and LDL cholesterol levels in ChD–wild-type mice were also significantly higher than those in normal diet–wild-type mice. High-density lipoprotein (HDL) cholesterol levels in ChD–apoE$^{-/-}$ mice
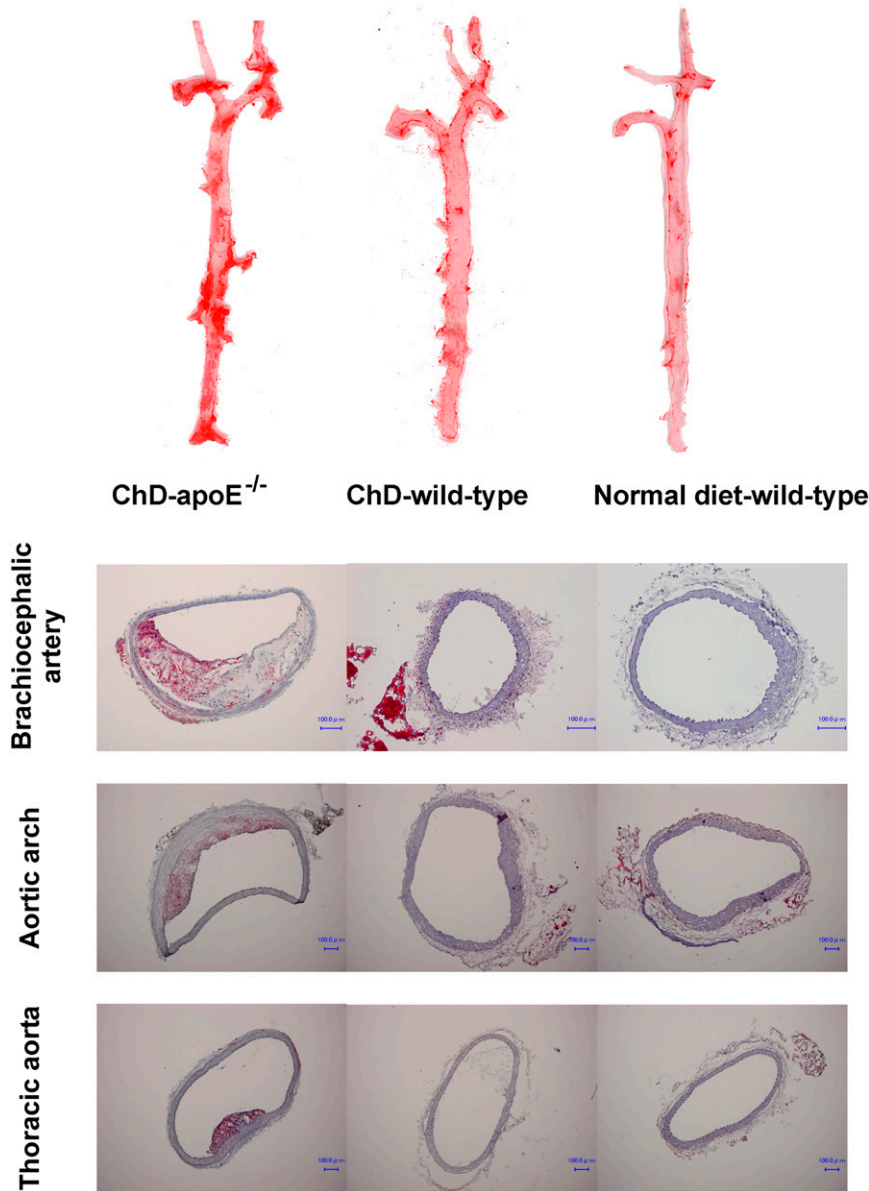
FIGURE 1. (Top) Examples of longitudinally incised aortas obtained from ChD–apoE$^{-/-}$, ChD–wild-type, and normal diet–wild-type mice and stained with Oil Red O (at age of 25 wk). Regions stained red with Oil Red O represent atherosclerotic lesions. (Bottom) Aortic tissues were also examined by cryostat sectioning at same age, and atherosclerotic plaques were confirmed histologically in ChD–apoE$^{-/-}$ mice but not in ChD–wild-type or normal diet–wild-type mice. Bar = 100 μm.

were significantly lower than those in ChD–wild-type and normal diet–wild-type mice for each age group. ChD–wild-type mice showed significantly higher HDL cholesterol levels than normal diet–wild-type mice. Blood glucose levels were stable in each treatment group of mice at different ages and were within normal ranges (Table 2). No significant differences were observed among treatment groups at each age, except for a significant but slight difference between ChD–apoE$^{-/-}$ mice and ChD–wild-type mice at 25 wk old.

Atherosclerotic Lesion Development

Early to histologically advanced atheromatous lesions were observed throughout the aortas of older ChD–apoE$^{-/-}$ mice. Advanced lesions (VP) were predominantly located in the brachiocephalic arteries and lesser curvature of the aortic arch. No atherosclerotic lesions were found in wild-type mice regardless of diet (ChD–wild-type mice and normal diet–wild-

type mice) (Fig. 1). Immunohistochemical staining with Mac-2 showed infiltration of macrophages in atherosclerotic plaques of ChD–apoE$^{-/-}$ mice but not ChD–wild-type or normal diet–wild-type mice (Supplemental Fig. 1).

Figure 2 shows a summary of atherosclerotic lesion development in ChD–apoE$^{-/-}$ mice as a percentage of total surface area occupied by regions positively stained with Oil Red O. In these mice, the total atherosclerotic lesion area increased significantly with age. No significant differences were noted in atherosclerotic lesion development between mice given ^{18}F-FDG and those given ^{99m}Tc-annexin A5.

Aortic Tracer Distribution

The aortic uptake of ^{18}F-FDG and ^{99m}Tc-annexin A5 is shown in Table 3. In normal diet–wild-type mice, the uptake of ^{18}F-FDG and ^{99m}Tc-annexin A5 remained unchanged throughout the experimental period. The level of aortic

TABLE 1
Body Weight and Serum Lipid Levels

Parameter	Mouse group	Mean ± SD in mice that were:		
		10 wk old	18 wk old	25 wk old
Body weight (g)	Normal diet–wild-type	21.34 ± 0.67	26.19 ± 1.77*	28.58 ± 1.58*†
	ChD–wild-type	26.92 ± 1.23‡	36.48 ± 3.13*‡	40.39 ± 3.28*†‡
	ChD–apoE$^{-/-}$	28.76 ± 2.02§	41.02 ± 6.57*‡	46.04 ± 5.35*§
Total cholesterol level (mg/dL)	Normal diet–wild-type	73.42 ± 5.58	68.50 ± 6.36	78.42 ± 11.84
	ChD–wild-type	143.00 ± 17.77‡	157.77 ± 18.51‡	179.38 ± 27.10*†‡
	ChD–apoE$^{-/-}$	1,386.17 ± 330.98‡§	2,097.00 ± 539.89*‡§	1,716.00 ± 383.81*†‡§
LDL cholesterol level (mg/dL)	Normal diet–wild-type	15.10 ± 5.53	12.52 ± 5.20	19.32 ± 4.31†
	ChD–wild-type	44.32 ± 12.33‡	59.34 ± 12.26*‡	73.65 ± 18.93*†‡
	ChD–apoE$^{-/-}$	1,358.22 ± 337.42‡§	2,056.33 ± 535.88*‡§	1,677.95 ± 375.12*†‡§
HDL cholesterol level (mg/dL)	Normal diet–wild-type	40.67 ± 2.15	42.10 ± 3.54	47.42 ± 7.20*
	ChD–wild-type	82.78 ± 11.67‡	88.54 ± 7.70‡	98.92 ± 11.41*†‡
	ChD–apoE$^{-/-}$	9.44 ± 4.25‡§	9.67 ± 2.15‡§	11.77 ± 3.27‡§

*$P < 0.05$ vs. 10-wk-old group.
†$P < 0.05$ vs. 18-wk-old group.
‡$P < 0.05$ vs. normal diet–wild-type group.
§$P < 0.05$ vs. ChD–wild-type group.

uptake of ^{18}F-FDG in ChD–wild-type mice increased progressively with age ($P < 0.0167$ for 10- vs. 18-wk-old mice and 18- vs. 25-wk-old mice), whereas that of ^{99m}Tc-annexin A5 reached a plateau at 18 wk and remained unchanged at 25 wk ($P < 0.0167$ for 10- vs. 18-wk-old mice). ChD–apoE$^{-/-}$ mice showed significantly higher levels of aortic uptake of ^{18}F-FDG and ^{99m}Tc-annexin A5 with age ($P < 0.0167$ for 10- vs. 18-wk-old mice and 18- vs. 25-wk-old mice for ^{18}F-FDG and 10- vs. 18-wk-old mice for ^{99m}Tc-annexin A5).

ChD–apoE$^{-/-}$ and ChD–wild-type mice showed significantly higher levels of aortic uptake of ^{18}F-FDG and ^{99m}Tc-annexin A5 than normal diet–wild-type mice at 18 and 25 wk. ChD–apoE$^{-/-}$ mice also tended to have higher levels of uptake of ^{18}F-FDG and ^{99m}Tc-annexin A5 than ChD–wild-type mice of the same age.

Correlation Between Atherosclerosis Progression and Aortic Tracer Accumulation

The surface area of the aorta that stained positively with Oil Red O was determined for ChD–apoE$^{-/-}$ mice after different periods of high-fat feeding. For both tracers, the aortic tracer uptake levels correlated directly with the progression of atherosclerosis ($r = 0.40$, $P = 0.03$, for mice given ^{18}F-FDG; $r = 0.46$, $P = 0.02$, for mice given ^{99m}Tc-annexin A5) (Fig. 3).

Correlation Between LDL Cholesterol Levels and Aortic Tracer Accumulation

Positive correlations were observed between LDL cholesterol levels and aortic tracer uptake levels in both mice given ^{18}F-FDG and mice given ^{99m}Tc-annexin A5 for each age group, except for 10-wk-old mice given ^{18}F-FDG (Supplemental Fig. 2).

DISCUSSION

To determine the effects of prolonged cholesterol loading on the aortic uptake of ^{18}F-FDG and ^{99m}Tc-annexin A5, we used the following models: apoE$^{-/-}$ mice fed a high-fat diet (ChD–apoE$^{-/-}$ mice), wild-type mice fed a high-fat diet (ChD–wild-type mice), and wild-type mice fed a regular chow diet (normal diet–wild-type mice).

Using these diets and different genetic backgrounds, we were able to separate mice into 3 distinct categories based on serum cholesterol levels or atherosclerotic status (Table 1;

TABLE 2
Blood Glucose Levels in Group Given ^{18}F-FDG

Mouse group	Glucose level (mg/dL, mean ± SD) in mice that were:		
	10 wk old	18 wk old	25 wk old
Normal diet–wild-type	141.67 ± 36.05	119.00 ± 11.47	121.00 ± 11.71
ChD–wild-type	122.67 ± 20.91	118.71 ± 26.23	139.53 ± 16.06
ChD–apoE$^{-/-}$	124.89 ± 42.59	122.83 ± 17.83	113.21 ± 18.0*

*$P < 0.05$ vs. ChD–wild-type group.

TABLE 3
Aortic Tracer Uptake Levels

Tracer	Mouse group	Aortic uptake level [(%ID × kg)/g, mean ± SD] in mice that were:		
		10 wk old	18 wk old	25 wk old
^{18}F-FDG	Normal diet–wild-type	0.054 ± 0.009	0.062 ± 0.008	0.053 ± 0.014
	ChD–wild-type	0.067 ± 0.019	0.099 ± 0.018*†	0.164 ± 0.093*†‡
	ChD–apoE$^{-/-}$	0.064 ± 0.016	0.145 ± 0.057*†	0.249 ± 0.124*†‡
^{99m}Tc-annexin A5	Normal diet–wild-type	0.021 ± 0.003	0.030 ± 0.005*	0.023 ± 0.003‡
	ChD–wild-type	0.026 ± 0.004†	0.037 ± 0.007*	0.036 ± 0.005*†
	ChD–apoE$^{-/-}$	0.029 ± 0.007†	0.042 ± 0.006*	0.047 ± 0.012*†§

*$P < 0.05$ vs. 10-wk-old group.
†$P < 0.05$ vs. normal diet–wild-type group.
‡$P < 0.05$ vs. 18-wk-old group.
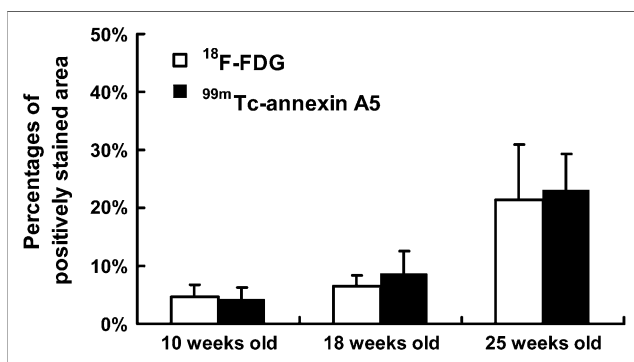§$P < 0.05$ vs. ChD–wild-type group.

Figs. 1 and 2). ChD–apoE$^{-/-}$ mice showed severe hypercholesterolemia, with extremely high serum LDL cholesterol levels, and all histologic grades of atherosclerotic disease. ChD–wild-type mice showed elevated serum LDL cholesterol levels but no histologic evidence of atherosclerotic disease. Normal diet–wild-type mice showed low serum cholesterol levels with increasing age and no evidence of atherosclerotic disease. These murine models also demonstrated different levels of aortic uptake of ^{18}F-FDG and ^{99m}Tc-annexin A5 (Table 3). For ChD–apoE$^{-/-}$ and ChD–wild-type mice, the levels of aortic accumulation of ^{18}F-FDG and ^{99m}Tc-annexin A5 tended to increase with age. A higher level of aortic uptake of each tracer was noted for ChD–apoE$^{-/-}$ mice than for age-matched ChD–wild-type mice. In the last model (normal diet–wild-type mice), the levels of aortic uptake of both ^{18}F-FDG and ^{99m}Tc-annexin A5 showed no significant change at any age. In addition, these values were significantly lower than the values obtained in ChD–wild-
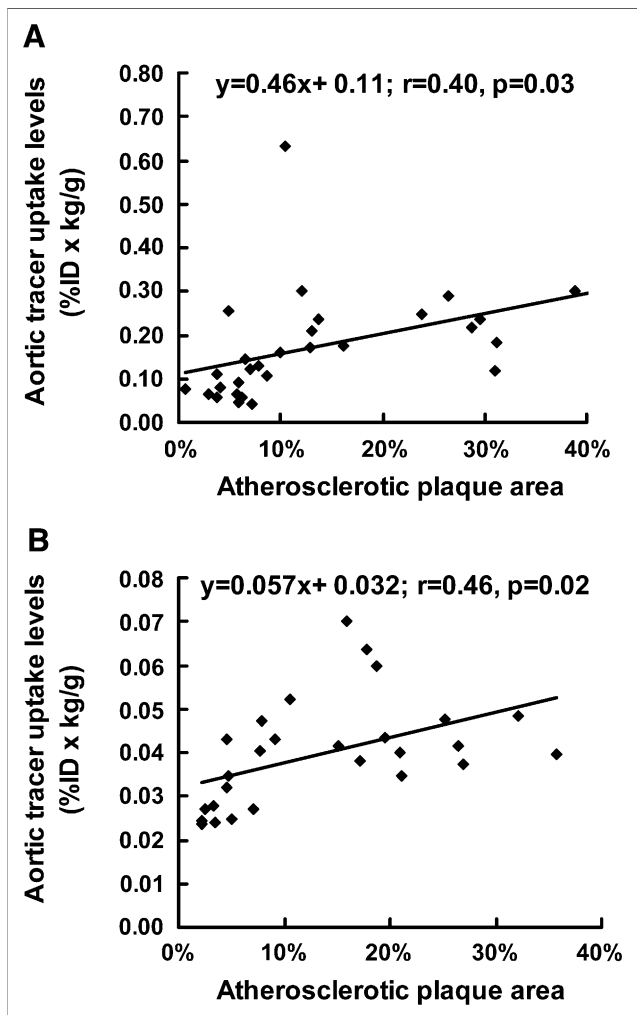

FIGURE 2. Percentages of surface area positively stained with Oil Red O in descending aorta of apoE$^{-/-}$ mice after different periods of high-fat feeding (ChD–apoE$^{-/-}$ mice). Percentages of positively stained surface area significantly increased with age ($F = 53.38$; $P < 0.001$). No significant differences were observed in percentages of positively stained area between groups given ^{18}F-FDG and ^{99m}Tc-annexin A5 ($F = 0.51$; $P = 0.48$).

type and ChD–apoE$^{-/-}$ mice. Our results indicated that the aortic uptake of ^{18}F-FDG and ^{99m}Tc-annexin A5 increased with the progression of atherosclerotic disease, underscoring the value of both tracers in the differential diagnosis of atherosclerosis. A caveat for the use of ^{18}F-FDG and ^{99m}Tc-annexin A5 in the diagnosis of atherosclerotic disease, however, is our observation that cholesterol feeding can actually increase the accumulation of these tracers in the aorta without any visible atheroma.

On the other hand, the uptake of ^{18}F-FDG and ^{99m}Tc-annexin A5 correlated directly with the extent of atherosclerotic lesions and the development of lesion severity in ChD–apoE$^{-/-}$ mice (Fig. 3), with uptake values absolutely higher than that in aging wild-type mice on either diet (Table 3). The uptake of ^{18}F-FDG and ^{99m}Tc-annexin A5 into atherosclerotic lesions and the correlation between tracer uptake levels and lesion vulnerability have also been confirmed by other experimental and clinical studies (20–25); our results are in agreement with those of previous investigations.

In addition to accelerating atherosclerosis in apoE$^{-/-}$ mice, high-fat feeding significantly increased plasma cholesterol levels and body weight in both apoE$^{-/-}$ and wild-type mice. These factors may also play important roles in the alteration of aortic tracer uptake. LDL cholesterol acts as a "bad cholesterol"; in particular, oxidized LDL cholesterol acts as a proinflammatory factor (8) that increases the levels of inflammatory mediators (9,10), decreases nitric oxide levels, and stimulates atherogenesis (26). Therefore, ChD–wild-type mice with elevated LDL cholesterol levels may in fact have chronic low-grade vascular inflammation. Older ChD–wild-type mice in our study were obese and had moderate hyperlipidemia. In previous investigations, C57BL/6J mice were used for the study of diet-induced obesity and diabetes (27–29). Furthermore, clinical investigations have shown that the plasma concentrations of tumor necrosis factor α, interleukin 6, C-reactive protein, and other inflammatory mediators are significantly elevated in obese individuals (30–32). Both lines of evidence suggest

FIGURE 3. Correlations between percentages of aortic surface area occupied by atherosclerotic plaques and aortic tracer uptake in ChD–apoE$^{-/-}$ mice. Correlations were calculated with linear regression analysis for groups given ^{18}F-FDG (A) and ^{99m}Tc-annexin A5 (B).

that there were elevated levels of inflammatory mediators in the ChD–wild-type mice used in the present study. Another line of evidence supporting our hypothesis was that described by Molnar et al. (*33*), who found that although high-fat feeding induced endothelial cell dysfunction, it did not enhance neointimal formation in C57BL/6J mice. In a recent clinical study, Yun et al. demonstrated that among several atherosclerosis risk factors (such as hypertension and diabetes), only hypercholesterolemia and age were consistently correlated with ^{18}F-FDG uptake levels in large arteries (*34*). Hypercholesterolemia expressed as high LDL levels may relate to the grade of vascular inflammation, and age representing the duration of cholesterol loading may also be required for delayed functional changes. In agreement with the results of Yun et al. (*34*), both total cholesterol and LDL levels and the duration of cholesterol loading played integral roles in driving aortic tracer uptake in the present study. When subjects underwent sufficiently pro-

longed cholesterol loading, the enhancement of aortic tracer uptake appeared to be associated with the severity of hypercholesterolemia. Assessment with the Spearman correlation coefficient by rank analysis indicated positive correlations between aortic tracer uptake and total cholesterol and LDL levels in both mice given ^{18}F-FDG and mice given ^{99m}Tc-annexin A5 for each age group, except for 10-wk-old mice given ^{18}F-FDG (Supplemental Fig. 2); however, a detailed correlation analysis could not be performed because of the large differences in LDL cholesterol levels between ChD–apoE$^{-/-}$ mice (>1,300 mg/dL) and wild-type mice (15–19 mg/dL for normal diet and 44–74 mg/dL for high-fat diet).

The duration of hypercholesterolemia is also an important factor. In the present study, prolonged high-fat feeding appeared to be necessary to change tracer uptake in the aorta. For example, although LDL cholesterol levels were 30-fold higher in ChD–apoE$^{-/-}$ mice than in ChD–wild-type mice at 10 wk (after 5 wk of cholesterol feeding), there were no significant differences in aortic tracer uptake. However, ChD–wild-type mice at 25 wk showed far lower LDL cholesterol levels but significantly higher levels of aortic tracer uptake than ChD–apoE$^{-/-}$ mice at 10 wk. Therefore, it is possible that the duration of cholesterol loading as opposed to the severity of hypercholesterolemia was the predominant factor driving tracer uptake.

With regard to HDL levels, Tahara et al. (*35*) demonstrated that the reduction in ^{18}F-FDG uptake was related to the enhancement of HDL levels with statin therapy for 3 mo. In contrast, the high-fat diet used in the present study increased not only LDL but also HDL levels in C57BL/6J mice, a result consistent with those of a previous report (*36*). The enhanced HDL levels did not prevent the increases in aortic tracer uptake in ChD–wild-type mice; therefore, no relationship was observed between aortic tracer uptake and HDL cholesterol levels in the present study. It has been reported that dietary effects on HDL levels are different in humans and mice. In humans, most cholesterol is carried in LDL, whereas mice carry most of their plasma cholesterol in HDL (*37*). Therefore, the relationship between tracer uptake and HDL levels and the species differences with regard to this point remain to be clarified.

It is known that ^{18}F-FDG is transported into aortic tissues through 2 types of glucose-transporting protein: Glut-1 and Glut-4 (*38–40*). Glut-1 is primarily responsible for the basal (i.e., insulin-independent) transport of glucose. Glut-4 is an insulin-sensitive glucose transporter that is greatly affected by blood insulin levels. Elevated blood glucose levels commonly enhance insulin levels and consequently increase ^{18}F-FDG as well as glucose accumulation in aortic tissues through Glut-4. In the present study, despite the higher blood glucose levels in ChD–wild-type mice than in ChD–apoE$^{-/-}$ mice at 25 wk (Table 2), ChD–apoE$^{-/-}$ mice still showed significantly higher levels of ^{18}F-FDG uptake in aortic tissues (Table 3). Accordingly, the slight difference in blood glucose levels observed in the present study appeared not to significantly affect aortic ^{18}F-FDG uptake.

In the present study, we could not apply dual-tracer techniques to measure aortic tracer uptake. Consequently, the aortic uptake of ^{18}F-FDG was determined separately from that of ^{99m}Tc-annexin A5 in different groups of mice; this study design prevented us from directly evaluating the correlation of the aortic uptake of the 2 tracers in the same animals. It is of great interest to determine the correlation between ^{18}F-FDG uptake and ^{99m}Tc-annexin A5 uptake, because both ^{18}F-FDG and ^{99m}Tc-annexin A5 are widely believed to be useful for the detection of unstable atheroma. Further studies with dual-tracer techniques are required for comparisons of ^{18}F-FDG uptake and ^{99m}Tc-annexin A5 uptake.

CONCLUSION

In the present study, we reported time-dependent changes in the aortic uptake of ^{18}F-FDG and ^{99m}Tc-annexin A5 in 3 murine models. After a prolonged high-fat diet, apoE$^{-/-}$ mice showed the highest levels of aortic uptake. Wild-type mice fed a high-fat diet showed higher aortic uptake levels than those fed a regular diet—but still lower than those of apoE$^{-/-}$ mice fed a high-fat diet. These findings indicate that not only the progression of atherosclerosis but also other proinflammatory factors, including prolonged cholesterol loading, alter the aortic uptake of ^{18}F-FDG and ^{99m}Tc-annexin A5. Tracer uptake should be assessed with caution in patients with proinflammatory risk factors, because the specificity for atherosclerotic disease may be adversely affected.

REFERENCES

1. Virmani R, Kolodgie FD, Burke AP, Farb A, Schwartz SM. Lessons from sudden coronary death: a comprehensive morphological classification scheme for atherosclerotic lesions. *Arterioscler Thromb Vasc Biol.* 2000;20:1262–1275.
2. Virmani R, Burke AP, Kolodgie FD, Farb A. Pathology of the thin-cap fibroatheroma: a type of vulnerable plaque. *J Interv Cardiol.* 2003;16:267–272.
3. Davies JR, Rudd JF, Fryer TD, Weissberg PL. Targeting the vulnerable plaque: the evolving role of nuclear imaging. *J Nucl Cardiol.* 2005;12:234–246.
4. Strauss HW, Grewal RK, Pandit-Taskar N. Molecular imaging in nuclear cardiology. *Semin Nucl Med.* 2004;34:47–55.
5. Lendon CI, Davies MJ, Born GV, Richardson PD. Atherosclerotic plaque caps are locally weakened when macrophage density is increased. *Atherosclerosis.* 1991;87:87–90.
6. Van der Wal AC, Becker AE, Van der Loss CM, Das PK. Site of intimal rupture or erosion of thrombosed coronary atherosclerotic plaques is characterized by an inflammatory process irrespective of dominant plaque morphology. *Circulation.* 1994;89:36–44.
7. Geng YJ, Libby P. Evidence for apoptosis in advanced human atheroma. *Am J Pathol.* 1995;147:251–266.
8. Boudjeltia KZ, Legssyer I, Van Antwerpen P, et al. Triggering of inflammatory response by myeloperoxidase-oxidized LDL. *Biochem Cell Biol.* 2006;84:805–812.
9. Libby P, Ridker PM. Inflammation and atherosclerosis: role of C-reactive protein in risk assessment. *Am J Med.* 2004;116(suppl 6A):9S–16S.
10. Ueland T, Vissers MN, Wiegman A, et al. Increased inflammatory markers in children with familial hypercholesterolaemia. *Eur J Clin Invest.* 2006;36:147–152.
11. Navab M, Imes SS, Hama SY, et al. Monocyte transmigration induced by modification of low density lipoprotein in cocultures of human aortic wall cells is due to induction of monocyte chemotactic protein 1 synthesis and is abolished by high density lipoprotein. *J Clin Invest.* 1991;88:2039–2046.
12. Xiao D, Wang Z, She M. Minimally modified low-density lipoprotein induces monocyte chemotactic protein-1 expression in vivo and a novel model for monocyte adhesion to arterial intima. *Chin Med J (Engl).* 1999;112:438–442.
13. Frostegard J, Nilsson J, Haegerstrand A, et al. Oxidized low density lipoprotein induces differentiation and adhesion of human monocytes and the monocytic cell line U937. *Proc Natl Acad Sci USA.* 1990;87:904–908.
14. Björkerud S, Björkerud B. Apoptosis is abundant in human atherosclerotic lesions, especially in inflammatory cells (macrophages and T cells), and may contribute to the accumulation of gruel and plaque instability. *Am J Pathol.* 1996;149:367–380.
15. Napoli C, Quehenberger O, De Nigris F, Abete P, Glass CK, Palinski W. Mildly oxidized low density lipoprotein activates multiple apoptotic signaling pathways in human coronary cells. *FASEB J.* 2000;14:1996–2007.
16. Colles SM, Maxson JM, Carlson SG, Chisolm GM. Oxidized LDL-induced injury and apoptosis in atherosclerosis: potential roles for oxysterols. *Trends Cardiovasc Med.* 2001;11:131–138.
17. Salvayre R, Auge N, Benoist H, Negre-Salvayre A. Oxidized low-density lipoprotein-induced apoptosis. *Biochim Biophys Acta.* 2002;1585:213–221.
18. Meir KS, Leitersdorf E. Atherosclerosis in the apolipoprotein E-deficient mouse: a decade of progress. *Arterioscler Thromb Vasc Biol.* 2004;24:1006–1014.
19. Mochizuki T, Kuge Y, Zhao S, et al. Detection of apoptotic tumor response in vivo after a single dose of chemotherapy with ^{99m}Tc-annexin V. *J Nucl Med.* 2003;44:92–97.
20. Zhao Y, Kuge Y, Zhao S, et al. Comparison of ^{99m}Tc-annexin A5 with ^{18}F-FDG for the detection of atherosclerosis in ApoE$^{-/-}$ mice. *Eur J Nucl Med Mol Imaging.* 2007;34:1747–1755.
21. Dunphy MP, Freiman A, Larson SM, Strauss HW. Association of vascular ^{18}F-FDG uptake with vascular calcification. *J Nucl Med.* 2005;46:1278–1284.
22. Ogawa M, Ishino S, Mukai T, et al. ^{18}F-FDG accumulation in atherosclerotic plaques: immunohistochemical and PET imaging study. *J Nucl Med.* 2004;45:1245–1250.
23. Kolodgie FD, Petrov A, Virmani R, et al. Targeting of apoptotic macrophages and experimental atheroma with radiolabeled annexin V: a technique with potential for noninvasive imaging of vulnerable plaque. *Circulation.* 2003;108:3134–3139.
24. Kietselaer BL, Reutelingsperger CP, Heidendal GA, et al. Noninvasive detection of plaque instability with use of radiolabeled annexin A5 in patients with carotid-artery atherosclerosis. *N Engl J Med.* 2004;350:1472–1473.
25. Isobe S, Tsimikas S, Zhou J, et al. Noninvasive imaging of atherosclerotic lesions in apolipoprotein E-deficient and low-density lipoprotein receptor–deficient mice with annexin A5. *J Nucl Med.* 2006;47:1497–1505.
26. Yla-Herttuala S. Oxidized LDL and atherogenesis. *Ann N Y Acad Sci.* 1999;874:134–137.
27. Survit RS, Kuhn CM, Cochrane C, McCubbin JA, Feinglos MN. Diet induced type II diabetes in C57BL/6J mice. *Diabetes.* 1988;37:1163–1167.
28. Survit RS, Seldin MF, Kuhn CM, Cochrane C, Feinglos MN. Control of expression of insulin resistance and hyperglycemia by different genetic factors in diabetic C57BL/6J mice. *Diabetes.* 1991;40:82–87.

29. Yamato M, Shiba T, Yoshida M, et al. Fatty acids increase the circulating levels of oxidative stress factors in mice with diet-induced obesity via redox changes of albumin. *FEBS J.* 2007;274:3855–3863.

30. Kern PA, Ranganathan S, Li C, Wood L, Ranganathan G. Adipose tissue tumor necrosis factor and interleukin-6 expression in human obesity and insulin resistance. *Am J Physiol Endocrinol Metab.* 2001;280:E745–E751.

31. Vozarova B, Weyer C, Hanson K, Tataranni PA, Bogardus C, Pratley RE. Circulating interleukin-6 in relation to adiposity, insulin action, and insulin secretion. *Obes Res.* 2001;9:414–417.

32. Pradhan AD, Manson JE, Rifai N, Bruing JE. Ridker PM. C-reactive protein, interleukin 6, and risk of developing type 2 diabetes mellitus. *JAMA.* 2001;286: 327–334.

33. Molnar J, Yu S, Mzhavia N, Pau C, Chereshnev I, Dansky HM. Diabetes induces endothelial dysfunction but does not increase neointimal formation in high-fat diet fed C57BL/6J mice. *Circ Res.* 2005;96:1178–1184.

34. Yun M, Yeh D, Araujo LI, Jang S, Newberg A, Alavi A. F-18 FDG uptake in the large arteries: a new observation. *Clin Nucl Med.* 2001;26:314–319.

35. Tahara N, Kai H, Ishibashi M, et al. Simvastatin attenuates plaque inflammation: evaluation by fluorodeoxyglucose positron emission tomography. *J Am Coll Cardiol.* 2006;48:1825–1831.

36. Smith JD, Breslow JL. The emergence of mouse models of atherosclerosis and their relevance to clinical research. *J Intern Med.* 1997;242:99–109.

37. Zhou J, Werstuck GH, Lhoták S, et al. Hyperhomocysteinemia induced by methionine supplementation does not independently cause atherosclerosis in C57BL/6J mice. *FASEB J.* 2008;22:2569–2578.

38. Pekala P, Marlow M, Heuvelman D, Connolly D. Regulation of hexose transport in aortic endothelial cells by vascular permeability factor and tumor necrosis factor-α, but not by insulin. *J Biol Chem.* 1990;265:18051–18054.

39. Atkins KB, Johns D, Watts S, Clinton Webb R, Brosius FC III. Decreased vascular glucose transporter expression and glucose uptake in DOCA-salt hypertension. *Hypertension.* 2001;19:1581–1587.

40. Standley PR, Rose KA. Insulin and insulin-like growth factor-1 modulation of glucose transport in arterial smooth muscle cells: implication of GLUT-4 in the vasculature. *Am J Hypertens.* 1994;7:357–362.